


## RESEARCH ARTICLE

# Do intrinsic brain functional networks predict working memory from childhood to adulthood?

Han Zhang<sup>1,2</sup>  | Shuji Hao<sup>2</sup> | Annie Lee<sup>1</sup> | Simon B. Eickhoff<sup>3,4</sup> |  
 Diliana Pecheva<sup>1</sup> | Shirong Cai<sup>5</sup> | Michael Meaney<sup>5</sup> | Yap-Seng Chong<sup>5,6</sup> |  
 Birit F. P. Broekman<sup>7</sup> | Marielle V. Fortier<sup>8</sup> | Anqi Qiu<sup>1,9</sup> 

<sup>1</sup>Department of Biomedical Engineering and Clinical Imaging Research Center, National University of Singapore, Singapore, Singapore

<sup>2</sup>School of Computer Engineering and Science, Shanghai University, Shanghai, China

<sup>3</sup>Institute for Systems Neuroscience, Medical Faculty, Heinrich-Heine University, Düsseldorf, Germany

<sup>4</sup>Institute of Neuroscience and Medicine (INM-7), Research Center Jülich, Jülich, Germany

<sup>5</sup>Singapore Institute for Clinical Sciences, Singapore, Singapore

<sup>6</sup>Department of Obstetrics and Gynaecology, Yong Loo Lin School of Medicine, National University of Singapore, Singapore, Singapore

<sup>7</sup>Department of Psychiatry, Amsterdam UMC, Location VU Medical Centre, VU University, Amsterdam, The Netherlands

<sup>8</sup>Department of Diagnostic and Interventional Imaging, KK Women's and Children's Hospital, Singapore, Singapore

<sup>9</sup>The N.1 Institute for Health, National University of Singapore, Singapore, Singapore

## Correspondence

Anqi Qiu, Department of Biomedical Engineering, National University of Singapore, 4 Engineering Drive 3, Block E4 #04-08, Singapore 117583, Singapore.  
 Email: bieqa@nus.edu.sg

## Funding information

Eunice Kennedy Shriver National Institute of Child Health and Human Development; National Institute on Drug Abuse; NUS Institute of Data Science; Ministry of Education; Agency for Science Technology and Research; Singapore Institute for Clinical Sciences; National Medical Research Council; Singapore National Research Foundation

## Abstract

Working memory (WM) is defined as the ability to maintain a representation online to guide goal-directed behavior. Its capacity in early childhood predicts academic achievements in late childhood and its deficits are found in various neurodevelopmental disorders. We employed resting-state fMRI (rs-fMRI) of 468 participants aged from 4 to 55 years and connectome-based predictive modeling (CPM) to explore the potential predictive power of intrinsic functional networks to WM in preschoolers, early and late school-age children, adolescents, and adults. We defined intrinsic functional networks among brain regions identified by activation likelihood estimation (ALE) meta-analysis on existing WM functional studies (ALE-based intrinsic functional networks) and intrinsic functional networks generated based on the whole brain (whole-brain intrinsic functional networks). We employed the CPM on these networks to predict WM in each age group. The CPM using the ALE-based and whole-brain intrinsic functional networks predicted WM of individual adults, while the prediction power of the ALE-based intrinsic functional networks was superior to that of the whole-brain intrinsic functional networks. Nevertheless, the CPM using the whole-brain but not the ALE-based intrinsic functional networks predicted WM in adolescents. And, the CPM using neither the ALE-based nor whole-brain networks predicted WM in any of the children groups. Our findings showed the trend of the prediction power of the intrinsic functional networks to cognition in individuals from early childhood to adulthood.

## KEYWORDS

brain connectome, brain development, neural fingerprint, resting-state fMRI, working memory

Han Zhang and Shuji Hao are joint first authors.

This is an open access article under the terms of the Creative Commons Attribution-NonCommercial License, which permits use, distribution and reproduction in any medium, provided the original work is properly cited and is not used for commercial purposes.

© 2020 The Authors. *Human Brain Mapping* published by Wiley Periodicals LLC.

## 1 | INTRODUCTION

Working memory (WM) is defined as the ability to maintain a representation online to guide goal-directed behavior (Baddeley, 1992). WM capacity is proven to increase significantly from early childhood to adolescence (Gathercole, Pickering, Ambridge, & Wearing, 2004; Ullman, Almeida, & Klingberg, 2014), and becomes relatively stable in adulthood (Eriksson, Vogel, Lansner, Bergström, & Nyberg, 2015; Nyberg et al., 2014). A substantial body of literature identifies the higher-order association cortex (e.g., frontal and parietal networks) to be associated with WM in late childhood (Crone & Steinbeis, 2017; Klingberg, Forssberg, & Westerberg, 2002; Ullman et al., 2014), adolescence (Finn, Sheridan, Kam, Hinshaw, & D'Esposito, 2010; Satterthwaite et al., 2013; Simmonds, Hallquist, & Luna, 2017), and adulthood (Constantinidis & Klingberg, 2016; Scherf, Sweeney, & Luna, 2006). WM capacity in early childhood predicts academic achievements in late childhood (Bull, Espy, & Wiebe, 2008; Cooper & Mackey, 2016) and deficits in WM are associated with neurodevelopmental disorders, such as attention-deficit/hyperactivity disorder (ADHD) and Autism Spectrum Disorders (Martinussen, Hayden, Hogg-Johnson, & Tannock, 2005; Wang et al., 2017). However, there is limited knowledge of neural substrates of WM in early childhood.

Recently, connectome-based predictive modeling (CPM) has been used to identify neural fingerprints from task-based and/or intrinsic brain functional networks that can robustly predict individuals' cognitive performance, such as general fluid intelligence (Finn et al., 2015), sustained attention (Rosenberg et al., 2015), working memory (Avery et al., 2019), and creative ability in adults (Beaty et al., 2018). The CPM employs the functional networks derived from sustained attention task fMRI data and predicts attention ability at the correlation of 0.8 in adults, while the CPM predictive power based on intrinsic resting-state functional networks is around 0.5 (Rosenberg et al., 2015). Similarly, the CPM using task-based functional networks predicts fluid intelligence at the correlation above 0.3, while the prediction of CPM using intrinsic functional networks to fluid intelligence is below 0.2 in adults (Greene, Siyuan, Scheinost, & Constable, 2018). These findings suggest that, to a certain degree, both task-based and intrinsic functional networks capture the significant variation of cognition observed in adults, with greater predictive power using task-based fMRI data. This may be partly because task-based functional networks encode specific cognitive processes and highlight the organization and coordination of brain regions involved in tasks. Moreover, Nostro et al. (2018) recently proposed to employ activation likelihood estimation (ALE) meta-analysis on existing task-functional studies to define brain regions that were consistently activated during specific cognitive processes (i.e., task-based ROIs) (Eickhoff et al., 2016; Rottschy et al., 2012). The intrinsic functional networks of these task-based ROIs can well predict individuals' personality traits (Nostro et al., 2018).

In this study, we adopted the above approaches and rs-fMRI data to investigate whether intrinsic functional networks of the whole brain or task-based ROIs derived from ALE can predict WM in preschoolers, early and late school-age children, adolescents, and adults based on

cross-sectional samples of 468 participants aged from 4 to 55 years. As the brain functional organization and WM capability undergo massive development in childhood and adolescence (Galván, 2017; Kaufmann et al., 2017; Ullman et al., 2014), we expected that brain functional networks involved in the prediction of the WM performance may differ among children, adolescents, and adults. This study constructed two types of intrinsic functional networks obtained from rs-fMRI: one among ROIs defined via ALE meta-analysis on existing WM-task functional studies and the other among 268 regions covering the whole brain. In detail, we applied ALE meta-analysis on existing WM-task functional studies (Eickhoff et al., 2016; Rottschy et al., 2012) to identify regions of activation relevant to WM. From rs-fMRI data, we defined intrinsic functional networks among these regions of activation (i.e., ALE-based intrinsic functional network). We then adopted the CPM prediction approach proposed in (Finn et al., 2015; Rosenberg et al., 2015) to predict the WM scores in preschoolers, early and late school-age children, adolescents, and adults, separately. Moreover, we conducted an exploratory analysis using intrinsic functional networks among the whole brain (i.e., whole-brain intrinsic functional networks) and examined their potential predictability to the WM score in these five age groups using the CPM. To evaluate the CPM prediction power, we employed another machine learning approach, relevance vector regression (RVR). Unlike the CPM, the RVR is a multivariate approach that is derived based on support vector regression and formulated in a Bayesian framework with sparseness constraint (Tipping, 2001). We chose the RVR in comparison with the CPM because it was previously applied to neuroimage data and showed its prediction power for language processing, spatial orientation-related skills, and personality (Cui & Gong, 2018; Nostro et al., 2018). We expected that this study could provide neural fingerprints based on the intrinsic functional networks for working memory development across the course from early childhood to adulthood.

## 2 | MATERIALS AND METHODS

### 2.1 | Participants

The institutional review boards at the institutions contributing to the four datasets approved all experimental and consenting procedures. The written consent was obtained from caregivers who came to the visit, and oral consent was obtained from children.

This study included four datasets obtained from the Growing Up in Singapore Towards healthy Outcomes (GUSTO) longitudinal birth cohort (Qiu et al., 2017; Wee et al., 2018), the Cognition and Brain Development in Children (CBDC) study (Zhong et al., 2014), the Pediatric Imaging, Neurocognition, and Genetics (PING) database (Jernigan et al., 2016, <http://ping.chd.ucsd.edu/>), and the Brain and Cognition Aging Study (BCAS) (Lee, Archer, Wong, Chen, & Qiu, 2013; Lee, Ratnarajah, Tuan, Chen, & Qiu, 2015). Figure S1 displays a flow chart of the subject selection. In short, participants without WM assessment or with unusable WM scores caused by experimental program errors, etc., were excluded from this study. We also excluded participants

with (a) major illnesses/surgery (heart, brain, kidney, and lung surgery); (b) neurological or psychiatric disorders; (c) learning disability or attention deficit; (d) history of diabetes or obesity; (e) head injury with loss of consciousness; and/or (f) nonremovable metal objects on/in the body such as a cardiac pacemaker. Finally, we included 468 participants who had usable WM assessment and satisfactory functional imaging data (i.e., rs-fMRI scans with maximal framewise displacement less than 0.5 mm and with more than 100 volumes scanning). As results, this study included 204 participants from the GUSTO study (4–6 years old), 110 from the CBDC study (6–10 years old), 95 from the PING study (10–21 years old), and 59 from the BCAS study (22–55 years old) according to all the criteria mentioned above. The age range was from 4 to 55 years. We assigned the participants into five age groups: preschoolers (4.5 ~ 4.69 years), early school-age children (5.84 ~ 6 years), late school-age children (6 ~ 10 years), adolescents (10.25 ~ 21 years), and adults (22 ~ 55 years). Table 1 lists the details of the data source, sample size, and age range of each age group.

## 2.2 | Working memory

In this study, we used the Spatial Working Memory (SWM) Task and the List Sorting Working Memory (LS) Test. Despite differences in protocol, both of these tasks are sequencing tasks (Baddeley, 2003) and have been proven to be effective for assessing working memory from childhood to adulthood (Akshoomoff et al., 2014; Faridi et al., 2015; Tulsy, Carlozzi, Chevalier, Beaumont, & Mugas, 2013; Waber et al., 2007).

### 2.2.1 | Spatial working memory task (SWM)

The Spatial Working Memory task from the Cambridge Neuropsychological Test Automated Battery (CANTAB) was used in the GUSTO, CBDC, and BCAS studies. The SWM is a computer-administered serial order pointing task in which participants search through an increasing number of boxes (from 4 to 8) to locate hidden blue tokens (Vance,

Ferrin, Winther, & Gomez, 2013). Children were administered a maximum of 6 boxes to avoid frustration and fatigue, while adults were given a maximum of 8 boxes (Faridi et al., 2015; Luciana & Nelson, 1998). Between-search errors are measured as the number of times participants revisit a box where a blue token has already been found. A higher score indicates poorer WM performance.

### 2.2.2 | List sorting working memory test (LS)

The List Sorting Working Memory Test from the NIH Toolbox Cognition Battery (NIHTB-CB) was used in the PING study. It requires participants to sort and sequence items illustrated by sequential pictures on the computer screen along with a recording of the name of the item (Tulsy et al., 2014). The score consists of the combined total of correct items on the 1- and 2-list conditions of the task (maximum 28 points). A higher score indicates better WM performance.

We standardized the SWM between-search errors and LS memory scores to make them comparable. In line with the LS memory score, we first inverted the SWM scores by subtracting them from the maximum score (i.e., 55) of the four age groups (preschoolers, early and late school-age children, and adults). Subsequently, we scaled each score into the range from 0 to 1 via  $(x_i - \min(x))/(\max(x) - \min(x))$ , where  $x_i$  was the WM score of each individual and  $x$  represented the WM scores of each age group. To be noted, the maximum and minimum scores for SWM and LS were defined respectively based on all age groups participating in SWM and LS. The standardized score was used in the below prediction model.

## 2.3 | MRI acquisition

The GUSTO, CBDC, and BCAS studies were conducted by the same group and their MRI acquisition protocols were comparable, while the PING study was conducted in multiple sites in the United States. We detailed the MRI acquisition for each study below.

**TABLE 1** Data information of five age groups

Data source	Age groups				
	Preschoolers	Early school-age children	Late school-age children	Adolescents	Adults
	GUSTO	GUSTO	CBDC	PING	BCAS
MRI Scanner	3T Siemens Skyra scanner		3T Siemens Magnetom Trio Tim scanner	Multi-scanners	3T Siemens Magnetom Trio Tim scanner
T <sub>1</sub> MRI	TR = 2000 ms, TE = 2.08 ms			–	TR = 2,300 ms, TE = 1.90 ms
rs-fMRI	TR = 2,660 ms, TE = 27 ms		TR = 2,400 ms, TE = 27 ms	–	TR = 2,300 ms, TE = 25 ms
Sample size	87	117	110	95	59
Age range (years)	4.50–4.69	5.84–6.00	6.00–10.00	10.25–21.00	22.00–55.00
Age (mean ± SD)	4.58 ± 0.05	5.94 ± 0.05	6.97 ± 1.04	16.79 ± 3.20	33.37 ± 10.84
Mean FWD (mean ± SD)	0.03 ± 0.02	0.04 ± 0.02	0.04 ± 0.02	0.06 ± 0.02	0.04 ± 0.02

Abbreviations: BCAS, the Brain and Cognition Aging Study; CBDC, the Cognition and Brain Development in Children project; FWD, frame-wise displacement; GUSTO, the Growing Up in Singapore Towards healthy Outcomes longitudinal birth cohort; PING, the Pediatric Imaging, Neurocognition, and Genetics database.

### 2.3.1 | GUSTO

Children underwent MRI scans using a 3 T Siemens Skyra scanner with a 32-channel head coil at KK Women's and Children's Hospital. The imaging protocols were: (a) high-resolution isotropic T1-weighted Magnetization Prepared Rapid Gradient Recalled Echo (MPRAGE; 192 slices, 1 mm thickness, in-plane resolution 1 mm, sagittal acquisition, field-of-view 192×192 mm, matrix = 192×192, repetition time = 2000 ms, echo time = 2.08 ms, inversion time = 877 ms, flip angle = 9°); (b) isotropic axial rs-fMRI protocol (single-shot echo-planar imaging; 48 slices with 3 mm slice thickness, no inter-slice gaps, matrix = 64 ×64, field-of-view = 192×192 mm, repetition time = 2,660 ms, echo time = 27 ms, flip angle = 90°, scan time = 5.27 min). The children were asked to close their eyes during the rs-fMRI scan.

To ensure image quality, children underwent MRI familiarity at home and on-site training programs prior to the MRI visit (Wen et al., 2017). Additionally, the image quality was verified immediately after the acquisition through visual inspection while children were still in the scanner. If there were motion artifacts (i.e., rings on the image, or blurring of structures) in MPRAGE, a repeated MPRAGE scan was conducted. The image was removed from the study if no acceptable image was acquired after three repetitions.

### 2.3.2 | CBDC

Children underwent MRI scans using a 3T Siemens Magnetom Trio Tim scanner with a 32-channel head coil at Clinical Imaging Research Centre of the National University of Singapore. The imaging protocols were: (a) high-resolution isotropic T1-weighted Magnetization Prepared Rapid Gradient Recalled Echo (MPRAGE; 190 slices, 1 mm thickness, in-plane resolution 1 mm, sagittal acquisition, field-of-view 190×190 mm, matrix = 190×190, repetition time = 2000 ms, echo time = 2.08 ms, inversion time = 850 ms, flip angle = 9°); (b) isotropic axial rs-fMRI protocol (single-shot echo-planar imaging; 42 slices with 3 mm slice thickness, no inter-slice gaps, matrix = 64×64, field-of-view = 190×190 mm, repetition time = 2,400 ms, echo time = 27 ms, flip angle = 90°, scan time = 6 min). The children were asked to close their eyes during the rs-fMRI scan.

### 2.3.3 | PING

The PING applied a standardized high-resolution MRI protocol involving 3D T1-weighted scans and gradient echo EPI scans for rs-fMRI. The PING MRI protocol for each scanner manufacturer is detailed at the website ([https://nda.nih.gov/edit\\_collection.html?id=2607](https://nda.nih.gov/edit_collection.html?id=2607)). The current analysis employed 95 subjects from the PING study whose MRI data were collected from two scanners (3T Siemens Magnetom Trio and 3T Philips Achieva). Repetition time for the Siemens scanner was 2,000 ms (scan time = 10 min) or 3,000 ms (scan time = 6.4 min), and repetition time for the Philips scanner was 2,500 ms (scan time = 6.5 min).

### 2.3.4 | BCAS

All adults were scanned using a 3T Siemens Magnetom Trio Tim scanner with a 32-channel head coil at the Clinical Imaging Research Centre of the National University of Singapore. The image protocols were: (a) high-resolution isotropic T1-weighted Magnetization Prepared Rapid Gradient Recalled Echo (MPRAGE; 192 slices, 1 mm thickness, sagittal acquisition, field of view 256×256 mm, matrix 256×256, repetition time 2,300 ms, echo time 1.90 ms, inversion time 900 ms, flip angle 9°); isotropic axial rs-fMRI imaging protocol (single-shot echo-planar imaging; 48 slices with 3 mm slice thickness, no inter-slice gaps, matrix 64 ×64, field of view 192×192 mm, repetition time 2,300 ms, echo time 25 ms, flip angle 90°, scanning time 8 min). During the rs-fMRI scan, the subjects were asked to close their eyes.

## 2.4 | MRI data analysis

MRI data from all datasets were processed in the same way as described below.

### 2.4.1 | Structural MRI

Anatomical segmentation into three tissue types, gray matter (GM), white matter (WM), and cerebrospinal fluid was performed using FreeSurfer 5.3.0 (Fischl et al., 2002). Postprocessing quality check was conducted according to the instruction on <https://surfer.nmr.mgh.harvard.edu/fswiki/FsTutorial/TroubleshootingData>. Nonlinear image normalization was achieved by aligning individual T1-weighted MRI images to the JHU atlas via large deformation diffeomorphic metric mapping (LDDMM) (Du, Younes, & Qiu, 2011; Tan & Qiu, 2016). The mapping accuracy of this method is superior to that in FreeSurfer and CARET (Du et al., 2011; Zhong, Phua, & Qiu, 2010).

### 2.4.2 | Rs-fMRI

The rs-fMRI data were preprocessed using FSL with slice time correction, motion correction, skull stripping, and intensity normalization. The rs-fMRI scans with maximal framewise displacement (FD) of head motion greater than 0.5 mm or with less than 100 volumes were removed from this study at this stage (Power, Barnes, Snyder, Schlaggar, & Petersen, 2012). Six motion parameters, white matter, cerebrospinal fluid, and global signals were further regressed out from rs-fMRI signals. Global signal regression (GSR) was performed to reduce artifactual variance due to head motion in pediatric, clinical, and elderly populations (Power et al., 2014). Band-pass filtering (0.01–0.08 Hz) was then applied. To align rs-fMRI data to the atlas, its mean functional volume was first aligned to the corresponding anatomical image via rigid-body alignment. The functional data were then transformed to the atlas space via LDDMM obtained based on the T<sub>1</sub>-weighted MRI.

## 2.5 | Intrinsic functional networks

### 2.5.1 | ALE-based intrinsic functional networks

ALE meta-analysis was used to identify brain regions that were consistently activated during WM tasks. Functional MRI or PET experiments related to WM in healthy participants were selected using BrainMap Sleuth 3.0 (Laird, 2009). Each experiment had a sample size greater than 5, participants with age less than 55 years old, and only positive activation. Based on these criteria, this study included 128 WM-task studies, 1972 subjects (93% of subjects were 21–55 years old), 144 experiments, and 3,528 brain foci (see Table S1). ALE meta-analysis in GingerALE 3.0 identified brain regions that were activated during WM processing (Eickhoff, Bzdok, Laird, Kurth, & Fox, 2012; Eickhoff, Laird, Fox, Lancaster, & Fox, 2017). The ALE map was thresholded at a cluster-forming threshold of  $p < .001$  and a cluster-level threshold of  $p < .05$  based on 1,000 permutations (Eickhoff et al., 2016; Eickhoff et al., 2017; Zhang et al., 2019), which formed the ALE-defined brain clusters (Figure 1). Finally, the ALE-defined brain clusters were parcellated into brain regions based on Shen's Atlas (Finn et al., 2015). Shen's atlas was created based on the functional connectivity and its brain parcellation is more suitable for studying rs-fMRI data (Finn et al., 2015). The regions that were very small or at the boundary of Shen's atlas parcels (i.e.,  $<500 \text{ mm}^3$ ) were excluded, resulting in 54 brain regions from the ALE-defined clusters. The ALE-based intrinsic functional networks among these 54 regions were constructed by calculating Pearson's correlation between the mean fMRI signals of any two seeds and Fisher's  $r$ -to- $z$  transformation.

### 2.5.2 | Whole-Brain intrinsic functional networks

We constructed whole-brain intrinsic functional networks based on the atlas that parcellated the whole brain into 268 regions (see Finn et al., 2015). Pearson's correlation coefficients between the mean fMRI signals of any two seeds were calculated and transformed to  $z$ -scores via Fisher's  $r$ -to- $z$  transformation.

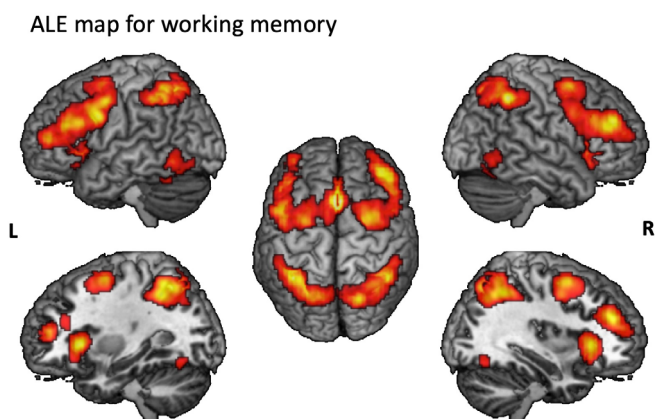


**FIGURE 1** The activation likelihood estimation (ALE) meta-analytic map for working memory. L, left; R, right

## 2.6 | Prediction models

### 2.6.1 | Connectome-Based predictive modeling

We performed the CPM (MATLAB syntax: <https://www.nitrc.org/projects/bioimagesuite/>) to predict WM performance based on the intrinsic functional networks in each age group (Shen et al., 2017). Given the sample size of this study, we employed five-fold cross-validation to evaluate the performance of the CPM (Scheinost et al., 2019; Varoquaux et al., 2017). We randomly divided all data into five folds in which four-folds served as a training dataset, and one fold served as a test dataset. In training, we calculated Spearman's rank correlation between WM score and each functional connectivity. Then, based on the absolute correlation coefficients, the top 100 WM-associated functional connectivities were selected as features. These features were further classified into connections positively and negatively associated with WM (i.e., WM correlated and anti-correlated networks). We then defined two total network strength scores: one as the sum of selected features in the WM positive correlated network; the other as the sum of the WM anticorrelated networks. We employed linear regression to fit the WM score as a function of the two total network strength scores (i.e., WM correlated and anticorrelated network strength) in the training dataset. In testing, we used this regression model to predict the WM score of the left-out fold. We evaluated the predictive power using Spearman's correlation between the observed and predicted WM scores. We repeated the fivefold cross-validation for 20 times to calculate the predictive power ( $r_s$ ) as the average correlation coefficient across 20 iterations. The  $p$ -value of Spearman's correlation was determined via the permutation test by randomly shuffling the WM score 1,000 times and by rerunning the above pipeline to create a null distribution of Spearman's correlation values in each age group. Empirical  $p$ -values were computed as  $(1 + \text{the number of permuted } r_s \text{ values greater than or equal to the empirical } r_s) / 1,001$ . This was carried out for both the ALE-based and whole-brain intrinsic functional networks.

The previous study indicated that the rs-fMRI functional network can well predict age ( $r$ -value ranges from 0.720 to 0.746) and gender (accuracy is 62%) (Casanova, Whitlow, Wagner, Espeland, & Maldjian, 2012; Dosenbach et al., 2010). As age and gender prediction is well studied (Casanova et al., 2012; Dosenbach et al., 2010), we conducted the additional analysis to predict age and gender using the same prediction model based on the whole-brain intrinsic functional networks across all the subjects in this study. This allows us to ensure that our prediction approach was not influenced due to the rs-fMRI processing, multi-sites, multi-scanners, and scanning time.

Also, we varied the number of functional connectivities used in the CPM, including (a) the top 50 functional connectivities that were most correlated with WM; (b) the functional connectivities that were significantly correlated with WM at  $p < .01$ . We repeated the CPM to predict the WM performance in each group.



## 2.6.2 | Relevance vector regression

We further employed relevance vector regression (RVR) to compare its prediction power with that of the CPM (Nostro et al., 2018; Tipping, 2001). Briefly, the RVR is a multivariate approach that was developed from the Support Vector Regression (SVR) to induce sparseness in the model parameters (Tipping, 2001). The feature selection for the RVR was the same as that in the CPM. Unlike the CPM, the RVR model directly took the selected features (e.g., the top 100 functional connectivities) as input features and estimated the probability of each of these features to predict the outcome measure in a probabilistic Bayesian framework (Tipping, 2001). Mathematically, the RVR model is more complex than the linear regression used in the CPM where only the two total network strength scores were used as independent variables. The RVR analysis followed the same cross-validation and evaluation approaches as those in the CPM analysis. In training, the RVR fitted the WM score as a function of the selected features (i.e., top 100 WM-associated connectivities). In testing, the estimated RVR model was used to predict the WM score of the left-out fold.

To ensure that the CPM and RVR predictions were not influenced by the head motion during rs-fMRI acquisition, we repeated the CPM and RVR (a) when the functional connectivity was computed via partial correlation with time-series FD as a covariate (Kaufmann et al., 2017); (b) when the mean FD across all time points was regressed out from the functional connectivity before the feature selection (Hsu, Rosenberg, Scheinost, Constable, & Chun, 2018).

## 3 | RESULTS

### 3.1 | Working memory

We first examined the group difference in WM across the five groups. The median WM scores were 0.49 in preschoolers, 0.61 in early school-age children, 0.71 in late school-age children, 0.77 in adolescents, and 0.82 in adults. Nonparametric Kruskal–Wallis ANOVA test revealed significant differences in WM among the five groups ( $p < .001$ ). The *post-hoc* analysis further revealed a significant increase in the WM performance from preschoolers, early and late school-age children, to adolescents ( $p < .001$ ). There was a marginally significant difference in WM between adolescents and adults ( $p = .079$ ). There were no significant correlations between the WM score and mean FD (head motion of rs-fMRI) in any age group ( $|r| < .125$ ,  $p > .19$ ) or across all the age groups ( $r = -.006$ ,  $p = .887$ ).

### 3.2 | Prediction of working memory from ALE-based intrinsic functional networks

Figure 1 shows the brain regions identified via ALE meta-analysis that were consistently activated during the WM processing. These brain

regions were mainly part of the frontoparietal, medial frontal, visual association cortex, and subcortical-cerebellar networks (see Figures 1 and 2a), which is consistent with that revealed by the meta-analysis on WM studies in Rottschy et al. (2012).

Figure 2b–f (orange lines) illustrate the top 100 functional connectivities selected during the feature selection stage for each age group. Figure 3a summarizes the number of these functional connections falling into one of 8 macroscale regions based on the atlas given in Finn et al. (2015). Visually, the functional connections of the medial frontal and frontoparietal networks with the subcortical-cerebellar, visual association, and motor networks were frequently selected as features in preschoolers. As age increased, these connections were still involved, however, the functional connections of the frontoparietal networks with the subcortical-cerebellar, visual association, and motor networks were increasingly selected (orange boxes in Figure 3a).

Based on the features shown in Figures 2 and 3, the CPM revealed that the ALE-based intrinsic functional networks did not significantly predict the WM score in preschoolers ( $r_s = .116$ ,  $p = .141$ ), early school-age children ( $r_s = -.082$ ,  $p = .706$ ), late school-age children ( $r_s = -.048$ ,  $p = .575$ ), and adolescents ( $r_s = -.016$ ,  $p = .487$ ) but predicted the WM performance in adults ( $r_s = .472$ ,  $p = .001$ ). Figure 4a illustrates the trend of the CPM predictive power to the WM score based on the ALE-based intrinsic functional networks from early childhood to adulthood.

### 3.3 | Prediction of working memory from Whole-Brain intrinsic functional networks

Figure 2b–f (cyan lines) illustrate the top 100 functional connectivities from the whole-brain intrinsic functional networks selected during the feature selection stage for each age group. In contrast to the ALE-based intrinsic functional networks, the functional connections selected from the whole-brain intrinsic functional networks as features involved more the subcortical-cerebellar connections but fewer the frontoparietal connections (Figure 3b,c) in children and adolescents. Nevertheless, most of these selected functional connections had one node belonging to the ALE-defined ROIs (50–70%), suggesting that the ALE-defined regions still play an important role in WM of children and adolescents. The features selected from both the ALE-based and whole-brain intrinsic functional networks are similar in adults (Figure 3b,c).

The CPM predictive power based on the whole-brain intrinsic functional networks was similar to that based on the ALE-based intrinsic functional networks (Figure 4b). The whole-brain intrinsic functional networks did not predict the WM score in preschoolers ( $r_s = .118$ ,  $p = .123$ ), early school-age children ( $r_s = .039$ ,  $p = .310$ ), and late school-age children ( $r_s = -.009$ ,  $p = .457$ ) but significantly predicted the WM score in adolescents ( $r_s = .228$ ,  $p = .034$ ) and adults ( $r_s = .312$ ,  $p = .008$ ). Nevertheless, the ALE-based intrinsic functional networks outperformed the whole-brain intrinsic

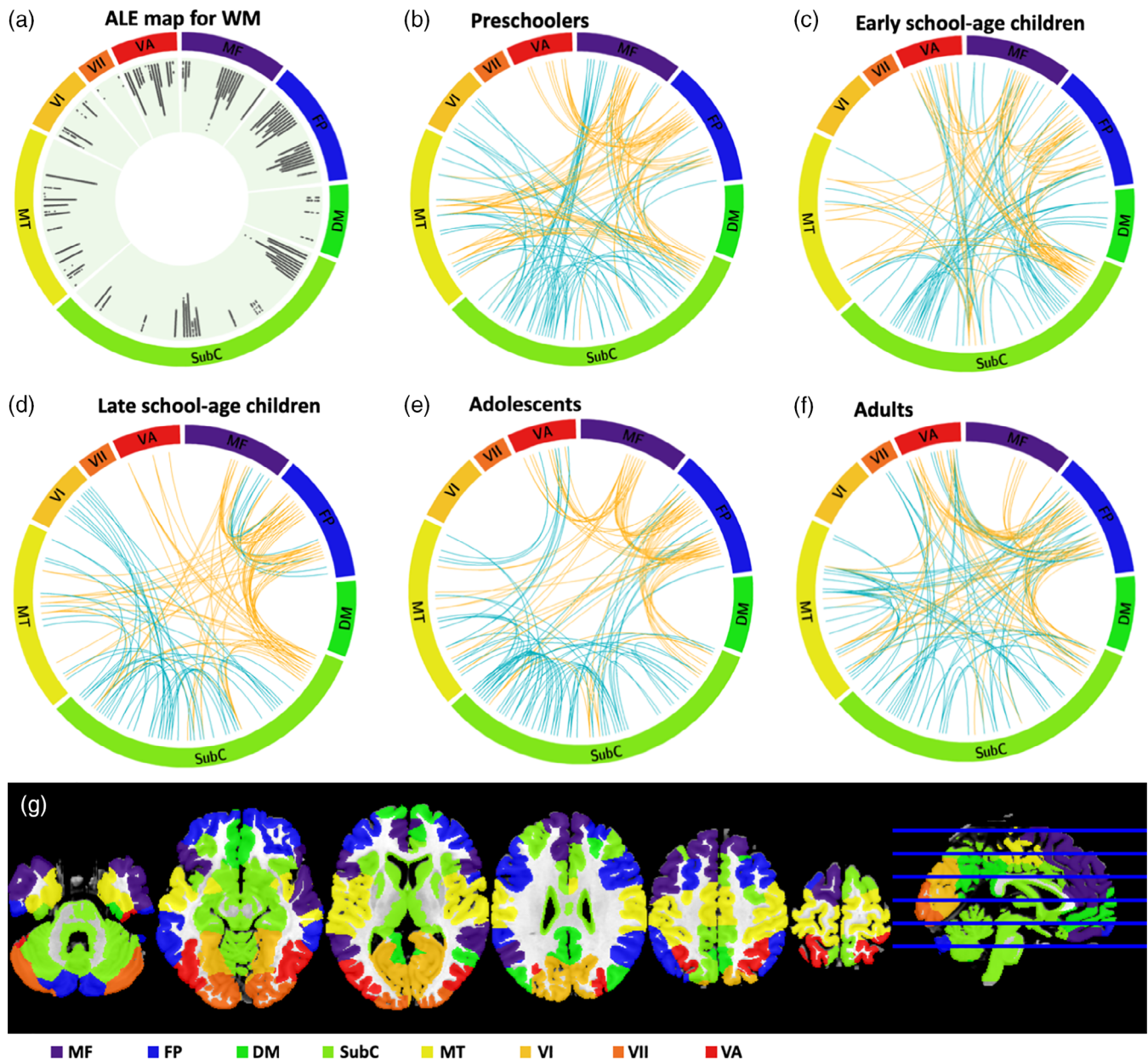


**FIGURE 2** The functional connectivities selected as features. Panel (a) indicates the ALE map for WM. From the outer to inner rings, the ALE values range from 0.01 to 0.13. A larger ALE value indicates that the region is more consistently activated in WM tasks across the existing fMRI-task studies. The ALE value is indicated by black line. The longer the line, the larger the ALE value. Panels (b–f) show the top 100 functional connections selected within each age group. Orange and cyan lines respectively show the top selected functional connections from the ALE-based and whole-brain intrinsic functional networks. Panel (g) illustrates the 8 macro-scale functional networks defined corresponding to the atlas given in Finn et al. (2015). DM, default mode; FP, frontoparietal; MF, medial frontal; MT, motor; SubC, subcortical-cerebellum; VI, visual I; VII, visual II; VA, visual association

functional networks for the WM prediction in adults ( $z = 34.589$ ,  $p < .001$ ; see Figure S2).

### 3.4 | The CPM and RVR comparison of the prediction Power

Analogous to the CPM, the RVR showed similar prediction patterns for each age group (see Table 2). Regardless of

whether the ALE-based or whole-brain intrinsic functional networks were used, the RVR did not predict the WM score in children but in adults. Similar to the CPM, the RVR can predict the WM score based on the whole-brain intrinsic functional networks but not based on the ALE-based intrinsic functional networks in adolescents. These results suggested that the predictive power from the ALE-based and whole-brain intrinsic functional networks did not vary with the classification approaches.

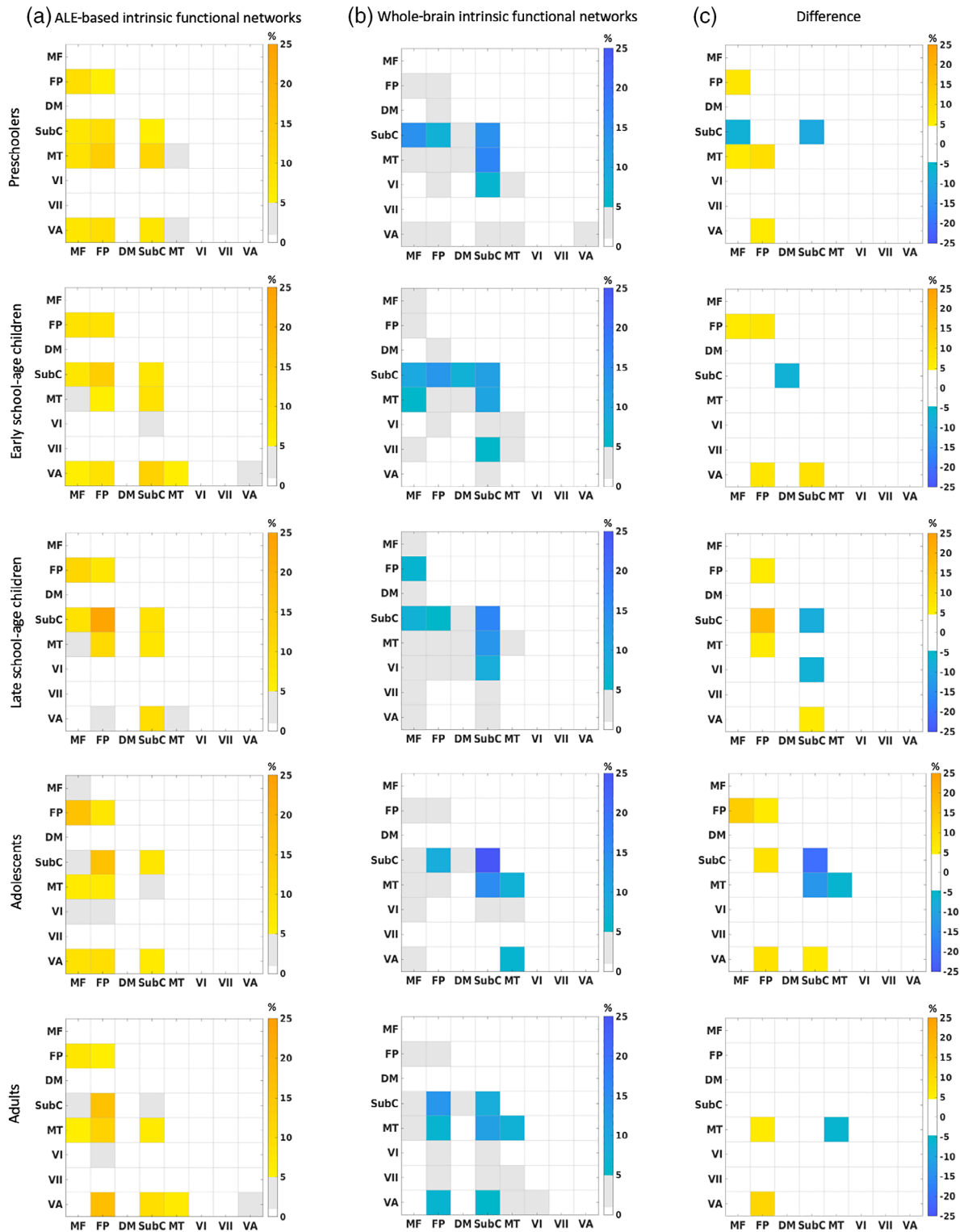


**FIGURE 3** The summary of the selected functional connectivities among the macroscale functional networks suggested in Finn et al. (2015). Columns (a) and (b) respectively illustrate the percentage of the functional connectivities selected from the ALE-based and whole-brain intrinsic functional networks as features. The color bar indicates the percentage of the selected connections over the total connections, where the selected connections have been consistently chosen across 20 iterations. Column (c) shows the difference between the corresponding panels in Columns (a) and (b). The orange blocks show the selected functional connections more from the ALE-based intrinsic functional networks, while cyan blocks show the selected functional connections more from the whole-brain intrinsic functional networks. DM, default mode; FP, frontoparietal; MF, medial frontal; MT, motor; SubC, subcortical-cerebellum; VI, visual I; VII, visual II; VA, visual association



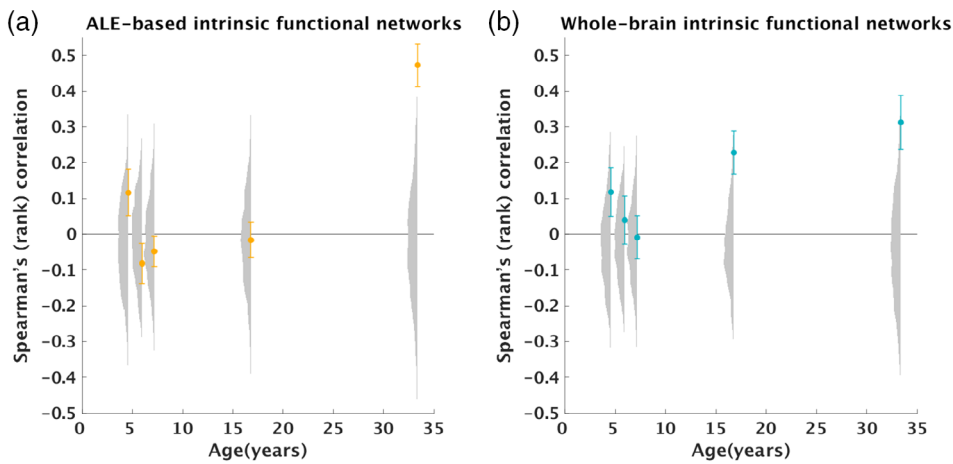


**FIGURE 4** The predictive power of the ALE-based (panel (a)) and whole-brain (panel (b)) intrinsic functional networks to working memory. The x-axis is the mean age of each age group, while the y-axis is the average Spearman's correlation coefficient  $r_s$  between the observed and predicted WM scores across iterations. The error bar shows the SD of the prediction power for each age group across 20 iterations. The null distributions of  $r_s$  from 1,000 permutation tests are shown in gray on each panel

	$r_s$ value (p value)				
	Preschoolers	Early school-age children	Late school-age children	Adolescents	Adults
<i>ALE-based intrinsic functional networks</i>					
CPM	.116 (.141)	-.082 (.706)	-.048 (.575)	-.016 (.487)	.472 (.001) <sup>a</sup>
RVR	.076 (.209)	-.143 (.892)	-.117 (.841)	-.065 (.641)	.510 (.001) <sup>a</sup>
<i>Whole-brain intrinsic functional networks</i>					
CPM	.118 (.123)	.040 (.310)	-.009 (.457)	.228 (.034) <sup>a</sup>	.312 (.008) <sup>a</sup>
RVR	.142 (.076)	.071 (.209)	-.021 (.488)	.210 (.027) <sup>a</sup>	.221 (.045) <sup>a</sup>

**TABLE 2** Prediction power of the intrinsic functional networks to working memory

Abbreviations: CPM, connectome-based predictive modeling; RVR, relevance vector regression.

<sup>a</sup>Significant predictive result according to 1,000 permutations.

### 3.5 | Potential effects of head motion and scanners

Figure 5 shows the CPM and RVR predictive power for WM scores for each age group after taking head motion into account in the calculation of the intrinsic functional connectivity (top row) and the feature selection of the functional connectivity (bottom row). Both strategies for controlling the head motion in CPM and RVR showed a similar predictive trend in each age group as shown in Figure 4. These findings suggested that the rs-fMRI head motion had limited effects on the CPM and RVR findings reported in the previous sections.

In our study, only the MRI data of adolescents were acquired using two scanners and the MRI acquisition of the rest of the age groups was done using the same scanner. We additionally rerun the CPM predictive modeling based on the whole-brain intrinsic functional networks in the adolescent group by accounting for the scanner effect. The result still showed the significance to predict WM in adolescents ( $r_s = .198$ ,  $p = .049$ ).

### 3.6 | Potential effects of feature selection in the CPM

Figure S3 shows the trend of the predictive power similar to that in Figure 4 when the top 50 functional connectivities or the functional

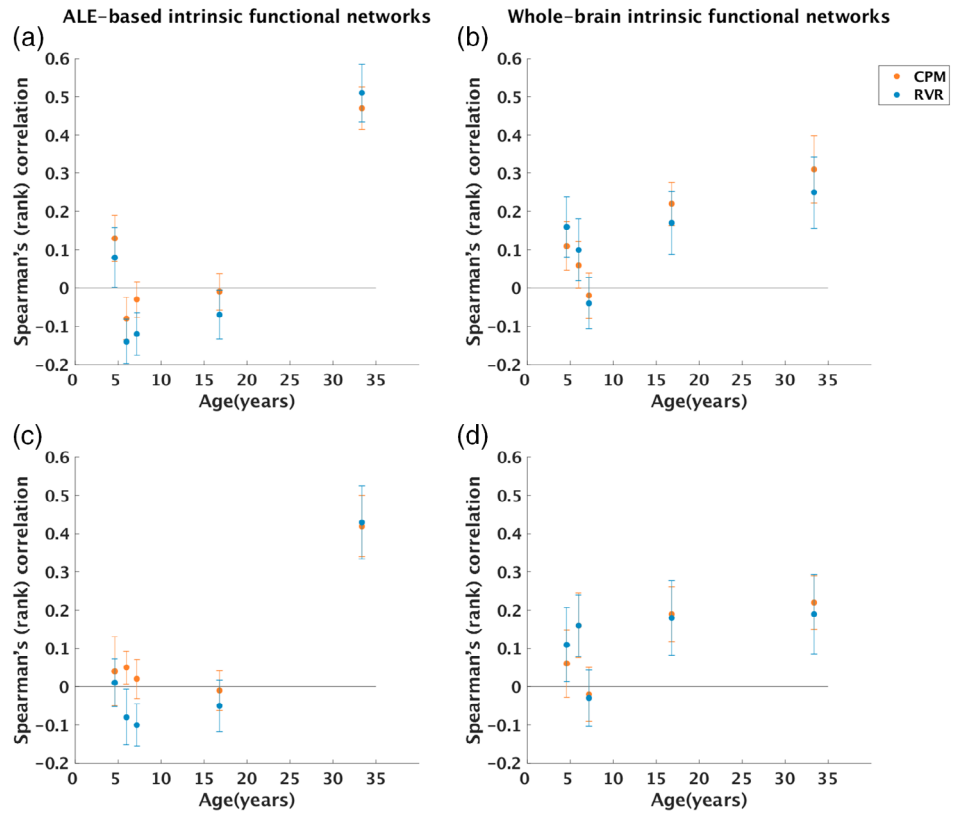
connectivities that were significantly associated with the WM performance at  $p < .01$  were used in CPM. This result suggested that the predictive power of CPM was not varied as a function of the number of functional connectivities used as features.

## 4 | DISCUSSION

This study demonstrates the possibility of the intrinsic brain functional networks in predicting the WM scores of individuals from early childhood to adulthood. Consistent with the previous findings (Greene et al., 2018; Rosenberg et al., 2015), both the intrinsic functional networks of the brain regions identified via ALE and whole-brain networks predicted adults' WM scores. In adolescents, the whole-brain but not ALE-based intrinsic functional networks predicted the WM scores. The ALE-based and whole-brain intrinsic functional networks did not predict children's WM scores. These findings may suggest that age-appropriate WM-activation maps are needed to improve the predictive power of the intrinsic functional networks for WM performance.

In this study, the prediction of the ALE-based and whole-brain intrinsic functional networks to WM in adults was mainly contributed by the functional connections of the frontoparietal network, specifically with the subcortical-cerebellar network. This is in line with the WM functional activation map in the prefrontal and parietal cortex,

**FIGURE 5** Head motion effects. Panels (a, b) respectively show the predictive power of the ALE-based and whole-brain intrinsic functional networks to working memory when the functional connectivity was computed via partial correlation with framewise displacement as a covariate. Panels (c, d) show the results when framewise displacement was regressed out from the functional connectivity before the feature selection



and subcortical structures in adults (Christophel, Hebart, & Haynes, 2012; Curtis & D'Esposito, 2003; Eriksson et al., 2015). Similar to recent studies (Avery et al., 2019; Greene et al., 2018; Rosenberg et al., 2015), the ALE-based and whole-brain intrinsic functional networks can well predict the WM performance of individual adults. The prediction power of the ALE-based intrinsic functional networks was superior to that of the whole-brain intrinsic functional networks (-Figure S2). These findings suggest that the prior knowledge of the brain regions involved in a specific cognition could be valuable for improving the prediction of individual cognitive ability in adults.

Unexpectedly, the whole-brain intrinsic functional networks were able to predict the WM score of individual adolescents but not the ALE-based intrinsic functional networks. This could be due to the difference in the features selected from the whole-brain and ALE-based networks (Figures 2 and 3). The features selected from the ALE-based networks were mainly anchored in the frontal cortex, while those from the whole-brain intrinsic functional networks were mainly in the subcortical-cerebellar connections. The involvement of the subcortical and cerebellar regions in the WM activation in adolescents has been previously reported (Darki & Klingberg, 2015; Eriksson et al., 2015), while the frontoparietal regions have been emphasized in the WM task in adults (Eriksson et al., 2015; Scherf et al., 2006). Furthermore, the CPM model trained using the ALE-based and whole-brain intrinsic functional networks of adults was not able to predict the WM score of the other age groups (see Table S2), indicating a potential difference of the neural circuits involved in the WM processing between adults and the rest of the age groups. Nevertheless, the functional organization of the brain is still ongoing during adolescence and has

not reached maturation (Simmonds et al., 2017). Given that our ALE meta-analysis was based predominantly on WM functional studies in adults, this may be a limiting factor in employing the ALE-based intrinsic functional networks to predict WM scores in adolescents. Hence, using age-appropriate WM-activation maps as a prior could improve the predictive power of individual cognitive performance.

Based on rs-fMRI, the brain intrinsic functional organization is diffuse in early childhood and becomes focal in adulthood (Casey, Tottenham, Liston, & Durston, 2005; Durston et al., 2006; Fair et al., 2008). Task-based WM studies also suggest that WM activations become more and more localized in the frontoparietal regions from childhood to adulthood (Crone & Steinbeis, 2017; Klingberg et al., 2002; Ullman et al., 2014). Hence, we expect that individual functional connectivities of the intrinsic functional networks might explain only a small variation of cognitive performance in children. This does not imply that providing WM-related brain regions as a prior in the CPM would not improve the prediction of WM in children. Further studies are needed to build a WM activation map tailored to children and determine the predictability of its intrinsic functional networks to WM.

This study incorporated the neuroimaging datasets of participants aged from early childhood to adulthood. Even though the sample size of adults in this study was the smallest, the predictive power of the intrinsic functional networks to WM was the strongest in adults. The children's neuroimaging cohorts in this study were relatively large, however, it is unclear whether increasing the sample size of children image data may improve the ability to predict WM. Also, similar to that in existing pediatric imaging studies (Barkovich, Xu, Desikan,

Williams, & Barkovich, 2018), the rs-fMRI scanning time of children in this study was relatively short (5–6 min) due to subjects' compliance in the scanner. Although short rs-fMRI scans well-predicted age (Dosenbach et al., 2010), further investigation may need to predict children's cognition using longer rs-fMRI scans. Moreover, the rs-fMRI datasets used in this study were acquired at several sites using different MRI scanners (Table 1). Previous studies showed that the study site, MRI scanner and the imaging protocol have limited effects on the predictive power of CPM (Horien et al., 2018; Noble et al., 2017). Split-half noise ceiling (SHnc) of rs-fMRI that quantifies the amount of fMRI noise did not differ in five groups (Lage-Castellanos, Valente, Formisano, & Demartino, 2019) (Figure S4). Hence, we would expect that these factors have only limited effects on our results. Our analysis did not show rs-fMRI head motion to have significant effects on the predictive power of CPM or RVR (Figure 5). This is most likely because we restricted our analysis to include only rs-fMRI data passing quality control. Furthermore, the whole-brain intrinsic functional networks can well predict subjects' age ( $r_s = .708$ ,  $p < .001$ ) as well as gender (accuracy = 62.33%,  $p < .001$ ) based on our current data (age range: 4 ~ 55 years), which is consistent with the literature (Casanova et al., 2012; Dosenbach et al., 2010). This suggests that our rs-fMRI processing and prediction approaches were reasonable and the aforementioned limitations, such as multi-sites, multi-scanners, scanning time, rs-fMRI preprocessing, and so on, were not major factors to influence the predictive power of the intrinsic functional networks. Last but not least, challenges in studying development lie in making comparable cognitive measures across all age groups, which may need large samples to overcome their variabilities across all age groups. Hence, our study would be considered as an initial investigation on the prediction of intrinsic brain functional networks in working memory from childhood to adulthood.

In summary, this study investigated the predictive power of intrinsic functional networks to WM from early childhood to adulthood. Our findings provide evidence on the possibility of intrinsic functional networks for the prediction of individual cognitive performance from childhood to adulthood. Age-appropriate functional activation maps may be needed to improve the ability of intrinsic functional networks to predict cognitive function, particularly in children and adolescents.

## ACKNOWLEDGMENTS

This research is supported by the Singapore National Research Foundation under its Translational and Clinical Research (TCR) Flagship Programme and administered by the Singapore Ministry of Health's National Medical Research Council (NMRC), Singapore—NMRC/TCR/004-NUS/2008; NMRC/TCR/012-NUHS/2014. Additional funding is provided by the Singapore Institute for Clinical Sciences, Agency for Science Technology and Research (A\*STAR), Singapore Ministry of Education (Academic research fund tier 1); NUHSRO/2017/052/T1-SRP-Partnership/01), and NUS Institute of Data Science, Singapore. PING is funded by the National Institute on Drug Abuse and the Eunice Kennedy Shriver National Institute of Child Health and Human Development. PING data are disseminated

by the PING Coordinating Center at the Center for Human Development, University of California, San Diego. The investigators within PING contributed to the design and implementation of PING and/or provided data but did not participate in analysis or writing of this report. A complete listing of PING investigators can be found at <https://www.chd.ucsd.edu/research/ping-study.html>.

## DATA AVAILABILITY STATEMENT

The data are available upon the request.

## ORCID

Han Zhang  <https://orcid.org/0000-0002-9348-6104>

Anqi Qiu  <https://orcid.org/0000-0002-0215-6338>

## REFERENCES

- Akshoomoff, N., Newman, E., Thompson, W. K., McCabe, C., Bloss, C. S., Chang, L., ... Jernigan, T. L. (2014). The NIH toolbox cognition battery: Results from a large normative developmental sample (PING). *Neuropsychology*, 28(1), 1–10. <https://doi.org/10.1037/neu0000001>
- Avery, E. W., Yoo, K., Rosenberg, M. D., Greene, A. S., Gao, S., Na, D. L., ... Chun, M. M. (2019). Distributed patterns of functional connectivity predict working memory performance in novel healthy and memory-impaired individuals. *Journal of Cognitive Neuroscience*, 32(2), 241–255. [https://doi.org/10.1162/jocn\\_a\\_01487](https://doi.org/10.1162/jocn_a_01487)
- Baddeley, A. (1992). Working memory. *Science*, 255(5044), 556–559. <https://doi.org/10.1126/science.1736359>
- Baddeley, A. (2003). Working memory: Looking back and looking forward. *Nature Reviews Neuroscience*, 4(10), 829–839. <https://doi.org/10.1038/nrn1201>
- Barkovich, M. J., Xu, D., Desikan, R. S., Williams, C., & Barkovich, A. J. (2018). Pediatric neuro MRI: Tricks to minimize sedation. *Pediatric Radiology*, 48, 50–55. <https://doi.org/10.1007/s00247-017-3785-1>
- Beaty, R. E., Kenett, Y. N., Christensen, A. P., Rosenberg, M. D., Benedek, M., Chen, Q., ... Silvia, P. J. (2018). Robust prediction of individual creative ability from brain functional connectivity. *Proceedings of the National Academy of Sciences*, 201713532, 1087–1092. <https://doi.org/10.1073/pnas.1713532115>
- Bull, R., Espy, K. A., & Wiebe, S. A. (2008). Short-term memory, working memory, and executive functioning in preschoolers: Longitudinal predictors of mathematical achievement at age 7 years. *Developmental Neuropsychology*, 33(3), 205–228. <https://doi.org/10.1080/87565640801982312>
- Casanova, R., Whitlow, C. T., Wagner, B., Espeland, M. A., & Maldjian, J. A. (2012). Combining graph and machine learning methods to analyze differences in functional connectivity across sex. *The Open Neuroimaging Journal*, 6, 1–9.
- Casey, B. J., Tottenham, N., Liston, C., & Durston, S. (2005). Imaging the developing brain: What have we learned about cognitive development? *Trends in Cognitive Sciences*, 9(3), 104–110. <https://doi.org/10.1016/j.tics.2005.01.011>
- Christophel, T. B., Hebart, M. N., & Haynes, J.-D. (2012). Decoding the contents of visual short-term memory from human visual and parietal cortex. *Journal of Neuroscience*, 32(38), 12983–12989. <https://doi.org/10.1523/JNEUROSCI.0184-12.2012>
- Constantinidis, C., & Klingberg, T. (2016). The neuroscience of working memory capacity and training. *Nature Reviews Neuroscience*, 17(7), 438–449. <https://doi.org/10.1038/nrn.2016.43>
- Cooper, E. A., & Mackey, A. P. (2016). Sensory and cognitive plasticity: Implications for academic interventions. *Current Opinion in Behavioral Sciences*, 10, 21–27. <https://doi.org/10.1016/j.cobeha.2016.04.008>

- Crone, E. A., & Steinbeis, N. (2017). Neural perspectives on cognitive control development during childhood and adolescence. *Trends in Cognitive Sciences*, 21(3), 205–215. <https://doi.org/10.1016/j.tics.2017.01.003>
- Cui, Z., & Gong, G. (2018). The effect of machine learning regression algorithms and sample size on individualized behavioral prediction with functional connectivity features. *NeuroImage*, 178(February), 622–637. <https://doi.org/10.1016/j.neuroimage.2018.06.001>
- Curtis, C. E., & D'Esposito, M. (2003). Persistent activity in the prefrontal cortex during working memory. *Trends in Cognitive Sciences*, 7(9), 415–423. [https://doi.org/10.1016/S1364-6613\(03\)00197-9](https://doi.org/10.1016/S1364-6613(03)00197-9)
- Darki, F., & Klingberg, T. (2015). The role of fronto-parietal and frontostriatal networks in the development of working memory: A longitudinal study. *Cerebral Cortex*, 25(6), 1587–1595. <https://doi.org/10.1093/cercor/bht352>
- Dosenbach, N. U. F., Nardos, B., Cohen, A. L., Fair, D. A., Power, J. D., Church, J. A., ... Schlaggar, B. L. (2010). Prediction of individual brain maturity using fMRI. *Science (New York, NY)*, 329(5997), 1358–1361. <https://doi.org/10.1126/science.1194144>
- Du, J., Younes, L., & Qiu, A. (2011). Whole brain diffeomorphic metric mapping via integration of sulcal and gyral curves, cortical surfaces, and images. *NeuroImage*, 56(1), 162–173. <https://doi.org/10.1016/j.neuroimage.2011.01.067>
- Durston, S., Davidson, M. C., Tottenham, N., Galvan, A., Spicer, J., Fossella, J. A., & Casey, B. J. (2006). A shift from diffuse to focal cortical activity with development. *Developmental Science*, 9(1), 1–20. <https://doi.org/10.1111/j.1467-7687.2005.00454.x>
- Eickhoff, S. B., Bzdok, D., Laird, A. R., Kurth, F., & Fox, P. T. (2012). Activation likelihood estimation meta-analysis revisited. *NeuroImage*, 59(3), 2349–2361. <https://doi.org/10.1016/j.neuroimage.2011.09.017>
- Eickhoff, S. B., Laird, A. R., Fox, P. M., Lancaster, J. L., & Fox, P. T. (2017). Implementation errors in the GingerALE software: Description and recommendations. *Human Brain Mapping*, 38(1), 7–11. <https://doi.org/10.1002/hbm.23342>
- Eickhoff, S. B., Nichols, T. E., Laird, A. R., Hoffstaedter, F., Amunts, K., Fox, P. T., ... Eickhoff, C. R. (2016). Behavior, sensitivity, and power of activation likelihood estimation characterized by massive empirical simulation. *NeuroImage*, 137, 70–85. <https://doi.org/10.1016/j.neuroimage.2016.04.072>
- Eriksson, J., Vogel, E. K., Lansner, A., Bergström, F., & Nyberg, L. (2015). Neurocognitive architecture of working memory. *Neuron*, 88(1), 33–46. <https://doi.org/10.1016/j.neuron.2015.09.020>
- Fair, D. A., Cohen, A. L., Dosenbach, N. U. F., Church, J. A., Miezin, F. M., Barch, D. M., ... Schlaggar, B. L. (2008). The maturing architecture of the brain's default network. *Proceedings of the National Academy of Sciences*, 105(10), 4028–4032. <https://doi.org/10.1073/pnas.0800376105>
- Faridi, N., Karama, S., Burgaleta, M., White, M. T., Evans, A. C., Fonov, V., ... Waber, D. P. (2015). Neuroanatomical correlates of behavioral rating versus performance measures of working memory in typically developing children and adolescents. *Neuropsychology*, 29(1), 82–91. <https://doi.org/10.1037/neu0000079>
- Finn, A. S., Sheridan, M. A., Kam, C. L. H., Hinshaw, S., & D'Esposito, M. (2010). Longitudinal evidence for functional specialization of the neural circuit supporting working memory in the human brain. *Journal of Neuroscience*, 30(33), 11062–11067. <https://doi.org/10.1523/JNEUROSCI.6266-09.2010>
- Finn, E. S., Shen, X., Scheinost, D., Rosenberg, M. D., Huang, J., Chun, M. M., ... Constable, R. T. (2015). Functional connectome fingerprinting: Identifying individuals using patterns of brain connectivity. *Nature Neuroscience*, 18(11), 1664–1671. <https://doi.org/10.1038/nn.4135>
- Fischl, B., Salat, D. H., Busa, E., Albert, M., Dieterich, M., Haselgrove, C., ... Dale, A. M. (2002). Whole brain segmentation: Automated labeling of neuroanatomical structures in the human brain. *Neuron*, 33(3), 341–355. [https://doi.org/10.1016/S0896-6273\(02\)00569-X](https://doi.org/10.1016/S0896-6273(02)00569-X)
- Galván, A. (2017). Adolescence, brain maturation and mental health. *Nature Neuroscience*, 20(4), 503–504. <https://doi.org/10.1038/nn.4530>
- Gathercole, S. E., Pickering, S. J., Ambridge, B., & Wearing, H. (2004). The structure of working memory from 4 to 15 years of age. *Developmental Psychology*, 40(2), 177–190. <https://doi.org/10.1037/0012-1649.40.2.177>
- Greene, A. S., Siyuan, G., Scheinost, D., & Constable, R. T. (2018). Task-induced brain state manipulation improves prediction of individual traits. *Nature Communications*, 2018, 2807. <https://doi.org/10.1038/s41467-018-04920-3>
- Horien, C., Noble, S., Finn, E. S., Shen, X., Scheinost, D., & Constable, R. T. (2018). Considering factors affecting the connectome-based identification process: Comment on Waller et al. *NeuroImage*, 169, 172–175. <https://doi.org/10.1016/j.neuroimage.2017.12.045>
- Hsu, W. T., Rosenberg, M. D., Scheinost, D., Constable, R. T., & Chun, M. M. (2018). Resting-state functional connectivity predicts neuroticism and extraversion in novel individuals. *Social Cognitive and Affective Neuroscience*, 13(2), 224–232. <https://doi.org/10.1093/scan/nsy002>
- Jernigan, T. L., Brown, T. T., Hagler, D. J., Akshoomoff, N., Bartsch, H., Newman, E., ... Dale, A. M. (2016). The pediatric imaging, neurocognition, and genetics (PING) data repository. *NeuroImage*, 124, 1149–1154. <https://doi.org/10.1016/j.neuroimage.2015.04.057>
- Kaufmann, T., Alnæs, D., Doan, N. T., Brandt, C. L., Andreassen, O. A., & Westlye, L. T. (2017). Delayed stabilization and individualization in connectome development are related to psychiatric disorders. *Nature Neuroscience*, 20(4), 513–515. <https://doi.org/10.1038/nn.4511>
- Klingberg, T., Forssberg, H., & Westerberg, H. (2002). Increased brain activity in frontal and parietal cortex underlies the development of visuospatial working memory capacity during childhood. *Journal of Cognitive Neuroscience*, 14(1), 1–10. <https://doi.org/10.1162/089892902317205276>
- Lage-Castellanos, A., Valente, G., Formisano, E., & Demartino, F. (2019). Methods for computing the maximum performance of computational models of fMRI responses. *PLoS Computational Biology*, 15(3), 1–25. <https://doi.org/10.1371/journal.pcbi.1006397>
- Laird, A. R. (2009). ALE meta-analysis workflows via the BrainMap database: Progress towards a probabilistic functional brain atlas. *Frontiers in Neuroinformatics*, 3, 1–11. <https://doi.org/10.3389/neuro.11.023.2009>
- Lee, A., Archer, J., Wong, C., Chen, S., & Qiu, A. (2013). Age-related decline in associative learning in healthy Chinese adults. *PLoS One*, 8, e80648. <https://doi.org/10.1371/journal.pone.0080648>
- Lee, A., Ratnarajah, N., Tuan, T. A., Chen, S. H. A., & Qiu, A. (2015). Adaptation of brain functional and structural networks in aging. *PLoS One*, 10(4), 1–16. <https://doi.org/10.1371/journal.pone.0123462>
- Luciana, M., & Nelson, C. A. (1998). The functional emergence of prefrontally-guided working memory systems in four- to eight-year-old children. *Neuropsychologia*, 36(3), 273–293. [https://doi.org/10.1016/S0028-3932\(97\)00109-7](https://doi.org/10.1016/S0028-3932(97)00109-7)
- Martinussen, R., Hayden, J., Hogg-johnson, S., & Tannock, R. (2005). A meta-analysis of working memory impairments in children with attention-deficit/hyperactivity disorder. *Journal of the American Academy of Child & Adolescent Psychiatry*, 44(4), 377–384. <https://doi.org/10.1097/01.chi.0000153228.72591.73>
- Noble, S., Scheinost, D., Finn, E. S., Shen, X., Papademetris, X., McEwen, S. C., ... Constable, R. T. (2017). Multisite reliability of MR-based functional connectivity. *NeuroImage*, 146(October 2016), 959–970. <https://doi.org/10.1016/j.neuroimage.2016.10.020>
- Nostro, A. D., Müller, V. I., Varikuti, D. P., Pläschke, R. N., Hoffstaedter, F., Langner, R., ... Eickhoff, S. B. (2018). Predicting personality from network-based resting-state functional connectivity. *Brain Structure*



- and Function, 223(6), 2699–2719. <https://doi.org/10.1007/s00429-018-1651-z>
- Nyberg, L., Andersson, M., Kauppi, K., Lundquist, A., Persson, J., & Pudas, S. (2014). Age-related and genetic modulation of frontal cortex efficiency. *Journal of Cognitive Neuroscience*, 26(4), 746–754. [https://doi.org/10.1162/jocn\\_a\\_00521](https://doi.org/10.1162/jocn_a_00521)
- Power, J. D., Barnes, K. A., Snyder, A. Z., Schlaggar, B. L., & Petersen, S. E. (2012). Spurious but systematic correlations in functional connectivity MRI networks arise from subject motion. *NeuroImage*, 59(3), 2142–2154. <https://doi.org/10.1016/j.neuroimage.2011.10.018>
- Power, J. D., Mitra, A., Laumann, T. O., Snyder, A. Z., Schlaggar, B. L., & Petersen, S. E. (2014). Methods to detect, characterize, and remove motion artifact in resting state fMRI. *NeuroImage*, 84, 320–341. <https://doi.org/10.1016/j.neuroimage.2013.08.048>
- Qiu, A., Shen, M., Buss, C., Chong, Y., Kwek, K., Saw, S., ... Fortier, M. V. (2017). Effects of antenatal maternal depressive symptoms and socioeconomic status on neonatal brain development are modulated by genetic risk. *Cerebral Cortex*, 27, 3080–3092. <https://doi.org/10.1093/cercor/bhx065>
- Rosenberg, M. D., Finn, E. S., Scheinost, D., Papademetris, X., Shen, X., Constable, R. T., & Chun, M. M. (2015). A neuromarker of sustained attention from whole-brain functional connectivity. *Nature Neuroscience*, 19(1), 165–171. <https://doi.org/10.1038/nn.4179>
- Rottschy, C., Langner, R., Dogan, I., Reetz, K., Laird, A. R., Schulz, J. B., ... Eickhoff, S. B. (2012). Modelling neural correlates of working memory: A coordinate-based meta-analysis. *NeuroImage*, 60(1), 830–846. <https://doi.org/10.1016/j.neuroimage.2011.11.050>
- Satterthwaite, T. D., Wolf, D. H., Erus, G., Ruparel, K., Elliott, M. A., Gennatas, E. D., ... Gur, R. E. (2013). Functional maturation of the executive system during adolescence. *Journal of Neuroscience*, 33(41), 16249–16261. <https://doi.org/10.1523/JNEUROSCI.2345-13.2013>
- Scheinost, D., Noble, S., Horien, C., Greene, A. S., Lake, E. M., Salehi, M., ... Constable, R. T. (2019). Ten simple rules for predictive modeling of individual differences in neuroimaging. *NeuroImage*, 193, 35–45. <https://doi.org/10.1016/j.neuroimage.2019.02.057>
- Scherf, K. S., Sweeney, J. A., & Luna, B. (2006). Brain basis of developmental change in visuospatial working memory. *Journal of Cognitive Neuroscience*, 18, 1045–1058. <https://doi.org/10.1162/jocn.2006.18.7.1045>
- Shen, X., Finn, E. S., Scheinost, D., Rosenberg, M. D., Chun, M. M., Papademetris, X., & Constable, R. T. (2017). Using connectome-based predictive modeling to predict individual behavior from brain connectivity. *Nature Protocols*, 12(3), 506–518. <https://doi.org/10.1038/nprot.2016.178>
- Simmonds, D. J., Hallquist, M. N., & Luna, B. (2017). Protracted development of executive and mnemonic brain systems underlying working memory in adolescence: A longitudinal fMRI study. *NeuroImage*, 157, 695–704. <https://doi.org/10.1016/j.neuroimage.2017.01.016>
- Tan, M., & Qiu, A. (2016). Large deformation multiresolution diffeomorphic metric mapping for multiresolution cortical surfaces: A coarse-to-fine approach. *IEEE Transactions on Image Processing*, 25(9), 4061–4074. <https://doi.org/10.1109/TIP.2016.2574982>
- Tipping, M. E. (2001). Sparse Bayesian learning and the relevance vector machine. *Journal of Machine Learning Research*, 1(3), 211–244. <https://doi.org/10.1162/15324430152748236>
- Tulsky, D. S., Carlozzi, N., Chevalier, N., Beaumont, J., & Mugas, D. (2013). NIH toolbox cognitive functioning battery: Measuring working memory. *Monographs of the Society for Research in Child Development*, 78(4), 70–87. <https://doi.org/10.1111/mono.12035>
- Tulsky, D. S., Carlozzi, N., Chiaravalloti, N. D., Beaumont, J. L., Kisala, P. A., Mungas, D., ... Gershon, R. (2014). NIH toolbox cognition battery (NIHTB-CB): List sorting test to measure working memory. *Journal of the International Neuropsychological Society*, 20(06), 599–610. <https://doi.org/10.1017/S135561771400040X>
- Ullman, H., Almeida, R., & Klingberg, T. (2014). Structural maturation and brain activity predict future working memory capacity during childhood development. *Journal of Neuroscience*, 34(5), 1592–1598. <https://doi.org/10.1523/JNEUROSCI.0842-13.2014>
- Vance, A., Ferrin, M., Winther, J., & Gomez, R. (2013). Examination of spatial working memory performance in children and adolescents with attention deficit hyperactivity disorder, combined type (ADHD-CT) and anxiety. *Journal of Abnormal Child Psychology*, 41(6), 891–900. <https://doi.org/10.1007/s10802-013-9721-4>
- Varoquaux, G., Raamana, P. R., Engemann, D. A., Hoyos-Idrobo, A., Schwartz, Y., & Thirion, B. (2017). Assessing and tuning brain decoders: Cross-validation, caveats, and guidelines. *NeuroImage*, 145, 166–179. <https://doi.org/10.1016/j.neuroimage.2016.10.038>
- Waber, D. P., De Moor, C., Forbes, P. W., Almli, C. R., Botteron, K. N., Leonard, G., ... Rumsey, J. (2007). The NIH MRI study of normal brain development: Performance of a population based sample of healthy children aged 6 to 18 years on a neuropsychological battery. *Journal of the International Neuropsychological Society*, 13(5), 729–746. <https://doi.org/10.1017/S1355617707070841>
- Wang, Y., Zhang, Y., Liu, L., Cui, J., Wang, J., Shum, D. H. K., ... Chan, R. C. K. (2017). A meta-analysis of working memory impairments in autism spectrum disorders. *Neuropsychology Review*, 27(1), 46–61. <https://doi.org/10.1007/s11065-016-9336-y>
- Wee, C., Poh, J. S., Wang, Q., Broekman, B. F., Chong, Y., Kwek, K., ... Qiu, A. (2018). Behavioral heterogeneity in relation with brain functional networks in young children. *Cerebral Cortex*, 28(9), 3322–3331. <https://doi.org/10.1093/cercor/bhx205>
- Wen, D. J., Poh, J. S., Ni, S. N., Chong, Y. S., Chen, H., Kwek, K., ... Qiu, A. (2017). Influences of prenatal and postnatal maternal depression on amygdala volume and microstructure in young children. *Translational Psychiatry*, 7(4), e1103. <https://doi.org/10.1038/tp.2017.74>
- Zhang, H., Wee, C.-Y., Poh, J. S., Wang, Q., Shek, L. P., Chong, Y.-S., ... Qiu, A. (2019). Fronto-parietal numerical networks in relation with early numeracy in young children. *Brain Structure and Function*, 224(1), 263–275. <https://doi.org/10.1007/s00429-018-1774-2>
- Zhong, J., Phua, D. Y. L., & Qiu, A. (2010). Quantitative evaluation of LDDMM, FreeSurfer, and CARET for cortical surface mapping. *NeuroImage*, 52, 131–141. <https://doi.org/10.1016/j.neuroimage.2010.03.085>
- Zhong, J., Rifkin-Graboi, A., Ta, A. T., Yap, K. L., Chuang, K. H., Meaney, M. J., & Qiu, A. (2014). Functional networks in parallel with cortical development associate with executive functions in children. *Cerebral Cortex*, 24(7), 1937–1947. <https://doi.org/10.1093/cercor/bht051>

## SUPPORTING INFORMATION

Additional supporting information may be found online in the Supporting Information section at the end of this article.

**How to cite this article:** Zhang H, Hao S, Lee A, et al. Do intrinsic brain functional networks predict working memory from childhood to adulthood? *Hum Brain Mapp*. 2020;41:4574–4586. <https://doi.org/10.1002/hbm.25143>